Synthesis, Characterisation, and Catalytic Activity of a Phosphinidene Stabilised Tethered Triruthenium Cluster†

Valentin D. Alexiev, Norman Binsted, Stephen L. Cook, John Evans,* and Richard J. Price
Department of Chemistry, The University, Southampton SO9 5NH
Nigel J. Clayden, Christopher M. Dobson, and Deborah J. Smith
Inorganic Chemistry Laboratory, South Parks Road, Oxford OX1 3QR
G. Neville Greaves
S.E.R.C. Daresbury Laboratory, Warrington WA4 4AD

A high-yield synthesis of $[Ru_3(\mu\text{-}H)_2(CO)_9\{\mu_3\text{-}PCH_2CH_2Si(OEt)_3\}]$ (**1**) from $[Ru_3(CO)_{12}]$ (**2**) has been developed. This complex can be tethered to high surface area oxide supports. The alumina based material has been characterised by i.r. and u.v.–visible spectroscopies and ^{31}P cross polarisation magic angle spinning n.m.r., all of which yield comparable data to that obtained for the precursor in solution. Comparison of the chemical shift anisotropy of (**1**)–alumina with that of a polycrystalline sample of $[Ru_3(\mu\text{-}H)_2(CO)_9(\mu_3\text{-}PPh)]$ (**3**) is consistent with (**1**) being firmly tethered to the oxide surface. Ruthenium *K*-edge extended *X*-ray absorption fine structure data were obtained for (**1**) and its alumina tethered version. Analysis of each required two Ru–Ru distances, as expected for the isosceles metal triangle in these complexes. For the tethered complex, these distances were 275(1) and 294(1) pm for the Ru–Ru and Ru–H–Ru units respectively.

Tethering transition metal carbonyl clusters to the surface of oxide powders has been of interest for some years as a method of preparing new heterogeneous catalysts.[1–6] However, the clusters appear to have limited stability on hydroxylated surfaces.[5,6] One possible way of circumventing this problem is to stabilise the cluster with a face-bridging ligand, and this has been demonstrated for the phosphinidene ligand.[7] We therefore aimed to synthesize the complex $[Ru_3(\mu\text{-}H)_2(CO)_9\{\mu_3\text{-}PCH_2CH_2Si(OEt)_3\}]$ (**1**) from $[Ru_3(CO)_{12}]$ (**2**) since closely related analogues were already known.[8] The tethering unit should present a less flexible unit than those commonly employed, which should also retard interactions with the surface. A brief report of part of this work has already appeared,[9] but since that time the characterisation of the tethered cluster has been improved. Two methods which have proven valuable for such materials are solid-state n.m.r.[10,11] and EXAFS (extended *X*-ray absorption fine structure)[12,13] and so both were applied to obtain more detail concerning the oxide supported clusters derived from complex (**1**).

Experimental

Infrared and u.v.–visible spectra were recorded on Perkin-Elmer 580B and 554 spectrometers respectively. Solution and solid-state n.m.r. spectra were obtained using Bruker AM360 and CXP200 spectrometers respectively. Ruthenium *K*-edge *X*-ray absorption spectra were recorded on Station 9.2 of the Synchrotron Radiation Source (S.R.S.) at the S.E.R.C. Daresbury Laboratory in transmission mode using a silicon (220) channel-cut monochromator. Two scans were made of each sample (*ca.* 1 h duration) and averaged. There was no evidence for radiation damage on comparing successive runs.

Diphenylphosphine,[14] $PPh(H)CH_2CH_2Si(OEt)_3$,[15] and $[Ru_3(CO)_{12}]$ (**2**)[16] were all prepared by published procedures.

Unless otherwise stated, reactions were performed under nitrogen.

† *Non-S.I. unit employed:* eV ≈ 1.60 × 10^{-19} J.

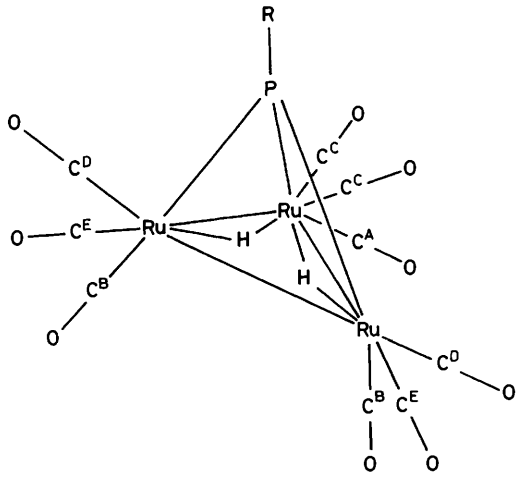

(**1**) R = $CH_2CH_2Si(OEt)_3$
(**3**) R = Ph

Reaction of $[Ru_3(CO)_{12}]$ (**2**) *with* PPh(H)R.—Compound (**2**) (0.5 g, 0.78 mmol) was dissolved in freshly distilled tetrahydrofuran (thf) (200 cm^3) and the phosphine PPh(H)R (0.93 mmol) [R = Ph or $CH_2CH_2Si(OEt)_3$] added. A solution of Na–Ph_2CO (0.01 mol dm^{-3} in thf) was added dropwise. After the addition of 5—10 drops the reaction solution darkened rapidly after which it was stirred for 40 min. The products were separated on a 2 × 15 cm flash chromatography silica column.[15,17] For R = $CH_2CH_2Si(OEt)_3$, elution with CH_2Cl_2–light petroleum (b.p. 40—60 °C) (1:1 v/v) afforded a mixture of $[Ru_3(\mu\text{-}H)(CO)_n\{\mu\text{-}P(Ph)CH_2CH_2Si(OEt)_3\}]$, n = 10 (**4**) or 9 (**5**), in 70% yield as an orange-yellow oil. For R = Ph elution with 10 and 20% v/v CH_2Cl_2–light petroleum (b.p. 40—60 °C) afforded $[Ru_3(CO)_{11}(PPh_2H)]$ (**6**) (dark red, 50%) and $[Ru_3(\mu\text{-}H)(CO)_{10}(\mu\text{-}PPh_2)]$ (**7**) (yellow, 10%).[18,19] I.r. ν(CO)

(cyclohexane): (**4**) at 2 098m, 2 053s, 2 047s, 2 019vs, 1 994m, and 1 988w cm^{-1}; (**5**) at 2 081m, 2 053s, 2 028s, 2 012m, 2 003w, 1 991w, and 1 984 cm^{-1}; (**6**) at 2 097m, 2 045s, 2 030s, 2 014vs, 1 996w, and 1 985w cm^{-1}. ^1H N.m.r. ($CDCl_3$): (**4**)/(**5**) δ 7.7 (m, 2 H, Ph), 7.02 (m, 3 H, Ph), 3.66 (q, 6 H, $MeCH_2O$–), 1.96 (m, 2 H, $–CH_2P$–), 1.07 (t, 9 H, Me), 0.72 (m, 2 H, $–SiCH_2$–), −16.36 [d, μ-H in (**4**), *J*(PH) 23 Hz], and −16.50 [d, μ-H in (**5**), *J*(PH) 28 Hz]; (**6**) δ 7.35 (m, 4 H, Ph), 6.95 (m, 6 H, Ph), and 6.45 [d, 1 H, P–H, *J*(PH) 365 Hz].

Preparation of $[Ru_3(\mu\text{-}H)_2(CO)_9(\mu_3\text{-}PR)]$ [R = $CH_2CH_2Si(OEt)_3$ (**1**) *or* Ph (**3**)].—The precursor complexes (**4**)/(**5**) [R = $CH_2CH_2Si(OEt)_3$] or (**6**) (R = Ph) (0.5 g) were heated in toluene (300 cm^3) at 80 °C under N_2 until conversion to $[Ru_3(\mu\text{-}H)(CO)_9(\mu\text{-}PPhR)]$ was complete. The solution was heated for a further 2 h under H_2, prior to product separation by flash chromatography. Products (**1**) and (**3**)[8] were obtained in 80—90% yield.

Complex (**1**). I.r. ν(CO) (cyclohexane): at 2 105m, 2 073s, 2 047vs, 2 028w, 2 015s, 1 997m, and 1 983w cm^{-1}. U.v.–visible (CH_2Cl_2): at 393, 287, and 230 nm. N.m.r. ($CDCl_3$): ^1H, δ 3.9 (q, 6 H, OCH_2), 3.1 (m, 2 H, PCH_2), 1.25 (t, 9 H, Me), 1.1 (m, 2 H, $SiCH_2$), and −19.26 [d, 2 H, μ-H, *J*(PH) 15 Hz]; $^{31}P\text{-}\{^1H\}$ (relative to H_3PO_4): δ 320.4 (s); $^{29}Si\text{-}\{^1H\}$ (relative to $SiMe_4$): δ −49.82 [d, *J*(SiP) 37 Hz]; ^{17}O (relative to H_2O): δ 22.7 (br, SiOEt), 351.2 (br, CO), and 372.7 (br, CO); $^{13}C\text{-}\{^1H\}$: δ *ca.* 191.1 (br, CO), 58.91 (s, OCH_2), 25.43 [d, PCH_2, *J*(PC) 55 Hz], 18.32 (s, Me), and 14.25 [d, $SiCH_2$, *J*(PC) 22 Hz].

Complex (**3**). $^{31}P\text{-}\{^1H\}$ N.m.r. (relative to H_3PO_4) (CH_2Cl_2): δ 282.7. ^{13}C N.m.r. (CH_2Cl_2 at −80 °C) (CO region): δ 200.72 [br d, 2 C, *J*(PC) 47 Hz], 195.24 [t or dd, 2 C, *J*(PC) 9 Hz], 191.06 [d of t, 1 C, *J*(PC) 44, *J*(HC) 4 Hz], 190.40 (s, 2 C), and 186.80 [dd, 2 C, *J*(HC) 9 and 4 Hz]; at 40 °C: δ 196.5 (br, 1 C) and 191 (br, 2 C); at 90 °C; δ 192.7 (br).

Protonation of Complex (**3**).—This was carried out by the addition of an excess of CF_3CO_2H to a solution of the complex in CD_2Cl_2,[20] giving the product $[Ru_3(\mu\text{-}H)_3(CO)_9(\mu_3\text{-}PPh)]^+$. N.m.r. ($CD_2Cl_2$–$CF_3CO_2H$): $^{31}P\text{-}\{^1H\}$: δ 267.7 (s); ^{13}C: δ 184.79 [dd, 3 C, C(axial), *J*(PC) 51, *J*(HC) 4 Hz] and 183.71 [m, 6 C, C(equatorial), *J*(PC) 6 Hz].

Interaction of (**1**) *with Oxides.*—A suspension of the oxide was stirred in a standard solution of (**1**) in CH_2Cl_2 in the (**1**):oxide ratio of 10:100 mg for 24 h at room temperature. The resulting solid was washed with CH_2Cl_2 and then acetone prior to drying *in vacuo*. The loading on the oxide was determined from quantification of the complex recovered from the washings.

Oxide = SiO_2. Loading of (**1**) 2.1%; i.r. ν(CO) (Nujol) at 2 107m, 2 071s, 2 045vs, 2 011m, and 1 995m cm^{-1}; u.v.–visible 393, 320, 287, and 230 nm.

Oxide = Al_2O_3. Loading of (**1**) 6.1%; i.r. ν(CO) (Nujol) at 2 104m, 2 070s, 2 043vs, 2 011m, 1 989m, and 1 969w cm^{-1}; u.v.–visible 404, 290, and 238 nm.

Oxide = TiO_2. Loading of (**1**) 3.1%; i.r. ν(CO) (Nujol) at 2 105m, 2 070s, 2 049 (sh), 2 042s, 2 013m, 1 988m, and 1 971w cm^{-1}; u.v.–visible: absorbing support.

Oxide = ZnO. Loading of (**1**) 2.3%; i.r. ν(CO) (Nujol) at 2 104m, 2 069s, 2 043vs, 2 011m, 1 985w (sh), and 1 973w cm^{-1}; u.v.–visible 416, 332, 300, and 230 nm.

Catalytic Studies on (**3**) *and* (**1**) *supported on Alumina.*—For the homogeneous catalysis, a solution of (**3**) (2 mg cm^{-3}) in CH_2Cl_2 (2 cm^3) with a pentene isomer (0.017 cm^3, 25 mol equiv.) was degassed and heated at the required temperature for 24 h. The volatile materials were separated from the residue by vacuum transfer and analysed using a Porasil C g.c. column containing 16% PhCN and 11% $AgNO_3$.[21] The heterogeneous catalysis was carried out in a similar manner using 85 mg of an alumina tethered sample of (**1**) with a loading of 4.47 mg (**1**):100 mg of Al_2O_3 suspended in CH_2Cl_2 (2 cm^3). In both regimes the cluster content was 4 mg (*ca.* 6×10^{-6} mol).

EXAFS Analysis.—The programs and procedures used were based on those described previously.[22] Background subtraction to afford the normalised Ru *K*-edge EXAFS proved difficult and a splined background routine was used.[23] Carbon and oxygen phase shifts were those used previously[22] and *ab initio* ruthenium phase shifts were calculated using the unperturbed atom as the model of both absorbing and scattering atom. This was based on the experience gained from fitting 4*d* metal *K*-edge EXAFS spectra.[24] Data analysis was using the program EXCURVE[25] on k^3-weighted EXAFS (k = photoelectron wave vector) over a data range of *ca.* 27—760 eV above E_0 (E_0 = photoelectron threshold energy difference from absorption). The proportion of absorption causing EXAFS was maintained at 0.8 and the co-ordination numbers held at their expected values. The shell radii, Debye–Waller factors, E_0 (*ca.* 17 eV), and the parameter VPI (*ca.* −4 eV) which models inelastic scattering of the photoelectron were all refined.

Results and Discussion

Synthesis and Characterisation of $[Ru_3(\mu\text{-}H)_2(CO)_9(\mu_3\text{-}PR)]$.—The simplest reaction to perform to yield the phenylphosphinidene cluster (**3**) is by the reaction of $PPhH_2$ and $[Ru_3(CO)_{12}]$. However, this affords a mixture of tri-,[8] tetra-,[26] and penta-nuclear[26] clusters and so would be inappropriate for synthesizing a cluster bearing a hydrolysable silyl group since this exacerbates purification problems. As an alternative, radical anion catalysis[27] was employed to introduce the phosphine onto the cluster. Since it has been demonstrated that hydrogenolysis of a PPh group in $[Ru_3(\mu\text{-}H)(CO)_9(\mu\text{-}PPh_2)]$ (**8**) can be used as a clean route to $[Ru_3(\mu\text{-}H)_2(CO)_9(\mu_3\text{-}PPh)]$,[18] secondary phosphines were used.

The Na–Ph_2CO catalysed substitution on $[Ru_3(CO)_{12}]$ by PPh_2H predominantly yielded a compound whose spectroscopic properties indicated it to be $[Ru_3(CO)_{11}(PPh_2H)]$ (**6**), together with a small proportion of $[Ru_3(\mu\text{-}H)(CO)_{10}(\mu\text{-}PPh_2)]$ (**7**).[18,19] The latter cluster can be reversibly decarbonylated at 50 °C to complex (**8**), the precursor to the phosphinidene stabilised species (**3**). Indeed, (**3**) can be prepared in high yield by sequentially decarbonylating and hydrogenating (**6**) in one vessel. The radical anion catalysed reaction between $[Ru_3(CO)_{12}]$ and $Ph(H)PCH_2CH_2Si(OEt)_3$ followed through to the cleavage of the P–H bond to form $[Ru_3(\mu\text{-}H)(CO)_n\{\mu\text{-}P(Ph)CH_2CH_2Si(OEt)_3\}]$, n = 10 (**4**) or 9 (**5**). These two complexes were not separable, but the relative proportions could be varied by heating solutions to 50 °C, either under CO to effect formation of (**4**), or under N_2 to yield (**5**) as the major species. The i.r. and n.m.r. properties of these two phosphido bridged clusters are as anticipated from comparison with the data observed on (**7**) and (**8**) respectively. Hydrogenolysis of the mixture could readily be effected at 80 °C, with the P–Ph bond being cleaved selectively in preference to the P–alkyl linkage. This could be anticipated from the comparable behaviour of triosmium complexes of alkyldiarylphosphines under thermolysis.[28] The result is a specific synthetic route to the complex $[Ru_3(\mu\text{-}H)_2(CO)_9\{\mu_3\text{-}PCH_2CH_2Si(OEt)_3\}]$ (**1**).

Complex (**1**) displayed similar i.r. absorptions in the C–O stretching region to those reported for its close analogue (**3**).[8] Its ^1H n.m.r. spectrum contained a ^{31}P split doublet at δ −19.26 due to the hydride protons, in addition to those features expected for the $–CH_2CH_2Si(OEt)_3$ chain. The integrity of this unit was confirmed by ^{13}C [which included two doublets with *J*(PC) values of 55 and 22 Hz due to the PCH_2CH_2Si chain],

^{17}O, and ^{29}Si n.m.r. The last resonance also displayed a phosphorus split doublet. The ^{31}P-$\{^1H\}$ spectrum consisted of one singlet 320.4 p.p.m. downfield of H_3PO_4. This is *ca.* 50 p.p.m. further downfield than the resonance of (**3**) but is in a characteristic region for phosphinidenes.

At room temperature, the ^{13}C n.m.r. features attributable to the carbonyl groups in both (**1**) and (**3**) are broad. A variable-temperature n.m.r. study of (**3**) was undertaken and this afforded a spectrum at −80 °C consisting of five ^{13}CO environments (relative intensities 2:2:2:2:1) as expected. The observed phosphorus and proton couplings indicate that the following assignments can be made: δ 200.72 (2 C^B), 195.24 (2 C^E), 191.06 (1 C^A), 190.40 (2 C^D), and 186.80 (2 C^C). Site exchange is evident above −40 °C and at 40 °C, a selective exchange process causes the carbonyl resonances to reduce to two signals (relative intensity 2:1), probably due to migration of the hydrides involving the vacant Ru–Ru edge; this gives a close match between the experimental and averaged chemical shifts. At higher temperatures there is total averaging which may be effected by the additional rotation about one or other of the $Ru(CO)_3$ groups.

The cluster (**3**) was protonated by trifluoroacetic acid to afford the cationic cluster $[Ru_3(\mu\text{-}H)_3(CO)_9(\mu_3\text{-}PPh)]^+$ (**9**) in which there is only the one ruthenium environment expected, co-ordinated to two edge-bridging hydrides.[20] Compared to complex (**3**), both the ^1H (of the hydride) and the ^{31}P resonances shift upfield on protonation (by 0.3 and 15 p.p.m. respectively). Under ambient conditions the ^{13}C n.m.r. spectrum of (**9**) contained two peaks in the carbonyl region, as expected for the axial (at higher frequency) and equatorial groups. [There is again an upfield chemical shift, generally associated for carbonyls with a decrease in the metal back-bonding. The axial resonance in the ^1H-coupled spectrum was observed as a doublet of doublets rather than the doublet of triplets expected for the C_{3v} geometry expected for (**9**).] This indicates that the localised rotation of an $Ru(CO)_3$ unit bound to two bridging hydrides is not rapid under ambient conditions, suggesting indeed that the low-temperature process in (**3**) is the hydride migration.

Interaction of (**1**) *with Oxides.*—Complex (**1**) was found to bind to samples of silica, alumina, titania, and zinc oxide with hydroxylated surfaces at room temperature. The loading of the cluster was oxide dependent, with alumina providing the highest value (6.1% w/w). The complex could not be removed from the oxide after Soxhlet extraction with CH_2Cl_2 overnight, indicating that the cluster is not merely physisorbed, and is more probably tethered *via* surface hydrolysis of the $-Si(OEt)_3$ group. The frequencies, band widths, and relative intensities of the C–O stretching absorptions in the i.r. agreed closely with those of a solution of (**1**) in CH_2Cl_2, consistent with the carbonyl containing species on the surface being a tethered derivative of (**1**). The diffuse-reflectance u.v.–visible spectrum of the alumina tethered derivative is also in good agreement with the absorption spectrum of the precursor in solution; on silica and zinc oxide there was an additional feature at *ca.* 320 nm suggesting partial decomposition.

Solid-state ^{31}P *N.M.R. of* (**3**) *and* (**1**)*–Alumina.*—The cross polarisation magic angle spinning (c.p.–m.a.s.) ^{31}P n.m.r. spectrum of a powdered sample of $[Ru_3(\mu\text{-}H)_2(CO)_9(\mu_3\text{-}PPh)]$ (**3**) is presented in Figure 1. The spectrum consists of three resonances, with isotropic chemical shifts of 273.5, 278.2, and 283.0 p.p.m. The centre-bands are flanked by side-bands spaced at the spinning frequency; the similar intensities of the three components of the latter indicate that their chemical shift anisotropies (c.s.a.s) are closely similar. The isotropic shifts are close to the ^{31}P chemical shift of 282.7 p.p.m. for (**3**) in CH_2Cl_2 solution. We attribute the reproducible occurrence of the three peaks to the existence of three crystallographically independent molecules of (**3**) in the unit cell.[8] These differ principally in the relative orientations of the phenyl group and the Ru_3 triangle. To check that the macroscopic sample possessed the same crystallographic characteristics as the single crystal previously studied, the experimental *X*-ray powder diffraction pattern was compared to that calculated from the single-crystal derived parameters.[29] This afforded satisfactory agreement.

The m.a.s. and static ^{31}P c.p. n.m.r. spectrum of (**1**)–alumina is presented in Figure 2. The isotropic chemical shift of 321.7

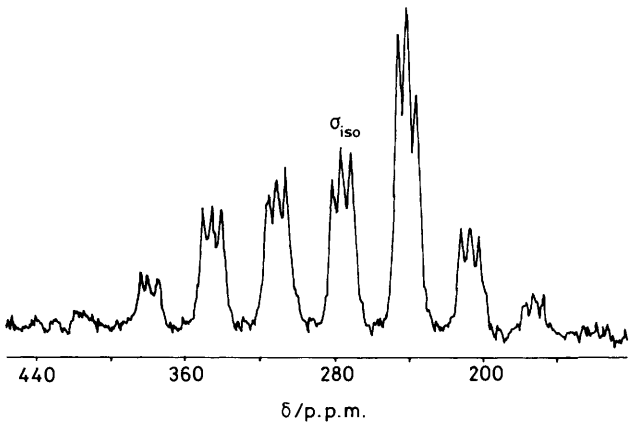

Figure 1. 80.96-MHz ^{31}P c.p.–m.a.s. n.m.r. spectrum of a powdered sample of $[Ru_3(\mu\text{-}H)_2(CO)_9(\mu_3\text{-}PPh)]$ (**3**). The sample was packed in a Delrin Andrew type rotor and spun at 2.8 kHz. 16 000 Scans were collected with the sample at 298 K using a sweep width of 50 kHz and a contact time of 1 s. The chemical shift is referenced to external 85% H_3PO_4, with downfield shift taken as positive. Moment analysis (M. M. Maricq and J. S. Waugh, *J. Chem. Phys.*, 1979, **70**, 3300) indicates $\sigma_\perp \simeq 190$ and $\sigma_\parallel \simeq 460$ p.p.m.

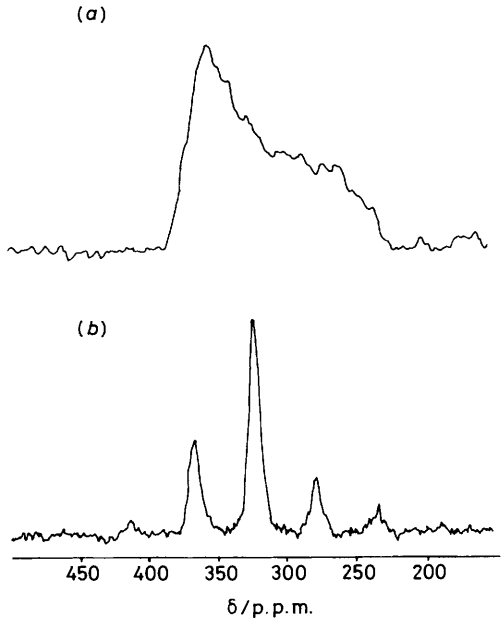

Figure 2. 80.96-MHz c.p.–m.a.s. n.m.r. spectra of (**1**)–alumina: (*a*) static spectrum and (*b*) m.a.s. recorded under similar conditions to those given with Figure 1, but with a spinning speed of 3.6 kHz. The powder spectrum indicates approximately axial symmetry of the shift tensor with $\sigma_\perp \simeq 370$ and $\sigma_\parallel \simeq 230$ p.p.m.

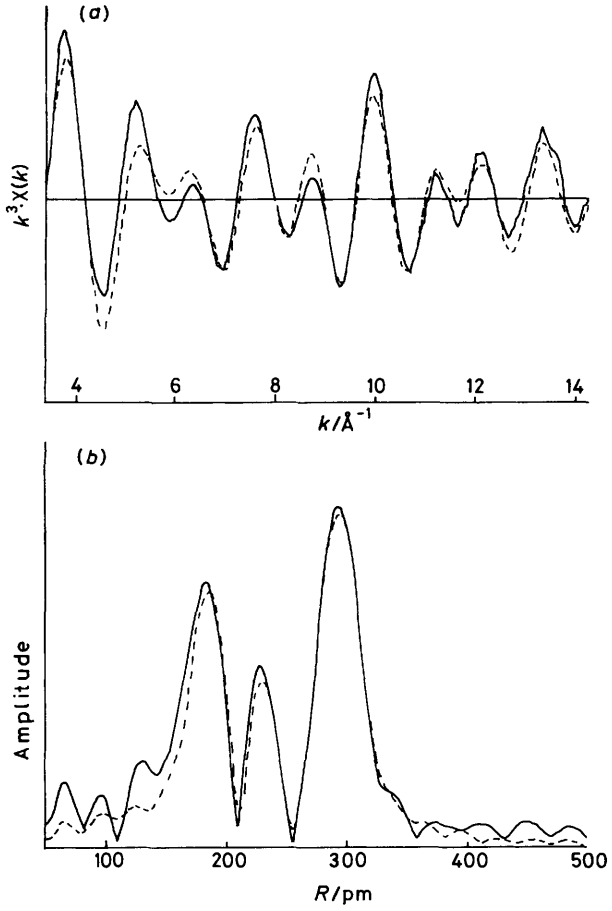

Figure 3. (*a*) k^3-Weighted Ru *K*-edge EXAFS of complex (**1**), and (*b*) its Fourier transform. Experimental (——) and calculated (– – –)

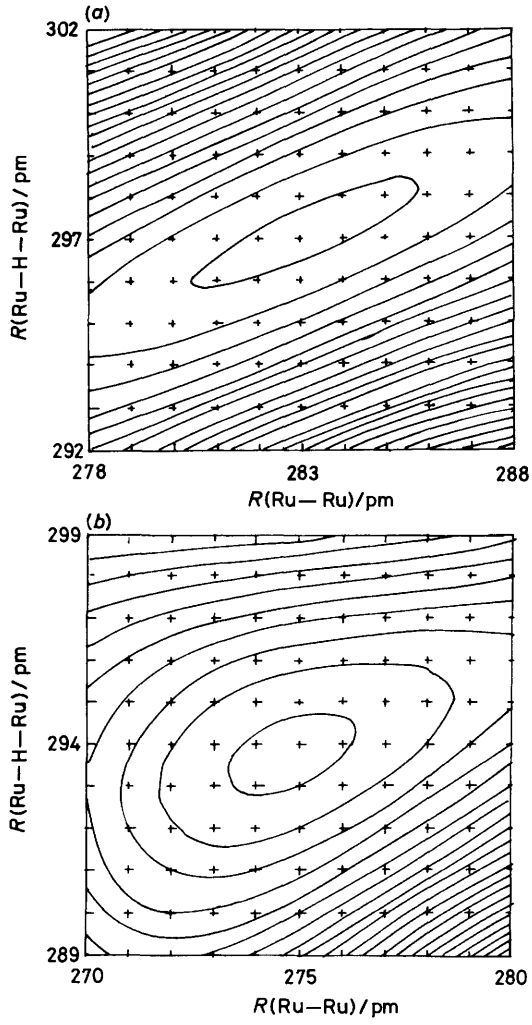

Figure 4. Contour maps of the fit index for the k^3-weighted Ru *K*-edge EXAFS for variations in the Ru–Ru and Ru–H–Ru interatomic distances. Minima are observed near the centre of the smallest contour rings. (*a*) Complex (**1**), lower contour 1.493, upper contour 9.486, increment 0.421; (*b*) complex (**1**)–alumina, lower contour 1.667, upper contour 10.121, increment 0.445

p.p.m. downfield of H_3PO_4 is within 2 p.p.m. of the chemical shift for complex (**1**) in solution. The rather broad line (*ca.* 700 Hz) is consistent with the previous results for surface attached species.[10,11] It can be attributed to a distribution of molecular environments on the surface; the spread of chemical shifts observed is in fact comparable to the differences in shift discussed above for the three molecules of (**3**) in the crystalline state. The static spectrum, also shown in Figure 2, shows an approximately axial shift tensor having the opposite sense to that observed for (**3**). The 50 p.p.m. isotropic shift difference on changing between an aryl and an alkyl group on the phosphinidene seems only to be an indication of the electronic changes at the phosphorus centre. The c.s.a. shows there are substantial and opposing shielding changes parallel and perpendicular to the principal magnetic axis, which is probably close to the P–C vectors. The substantial shift anisotropy of (**1**)–alumina indicates that fast motion with extensive angular fluctuations is not occurring on the surface.[11] The possibility of anisotropic rotation, for example about the short chain tethering the cluster to the surface, does exist and indeed would be consistent with the reduced anisotropy of the shift in the tethered cluster (**1**) compared to the crystalline cluster (**3**).

Ruthenium K-*edge EXAFS Studies on* $[Ru_3(CO)_{12}]$ (**2**), (**1**), *and* (**1**)–*Alumina*.—Before analysing the data on the more complicated phosphinidene species, $[Ru_3(CO)_{12}]$ (**2**) was used to test the precision of the calculated *ab initio* phase shifts and back-scattering factors. The results of this analysis are presented in Table 1. The co-ordination numbers were constrained to the crystallographic values and the Debye–Waller factors and interatomic distances refined for a three-shell model. The deviations in the Ru–C (+3 pm) and Ru–Ru (−3 pm) bond lengths from the mean of those determined by *X*-ray diffraction[30] represent an error of *ca.* 1%; this is approximately the precision expected from such analyses.

The Ru *K*-edge EXAFS of a sample of (**1**) diluted by boron nitride was analysed in a similar manner. The co-ordination numbers were maintained at values expected for a $[Ru_3H_2(CO)_9(\mu_3\text{-PR})]$ unit. No crystallographic study has been carried out for this complex, so the interatomic distances derived in this way are compared to those reported for complex (**3**) (R = Ph).[8] A five-shell model was ultimately used, with the experimental and the final fit theoretical EXAFS, and their Fourier transforms, presented as Figure 3. Three shells are evident in the Fourier transform. The two at lower *R* values are due to back-scattering associated with the Ru–C and Ru–P bond lengths; these values are within 1 pm of the crystallographic means for (**3**). The outermost radius shell was analysed as having three components, *viz.* the Ru–Ru and Ru–H–Ru intermetallic distances and the carbonyl Ru · · · O separation.

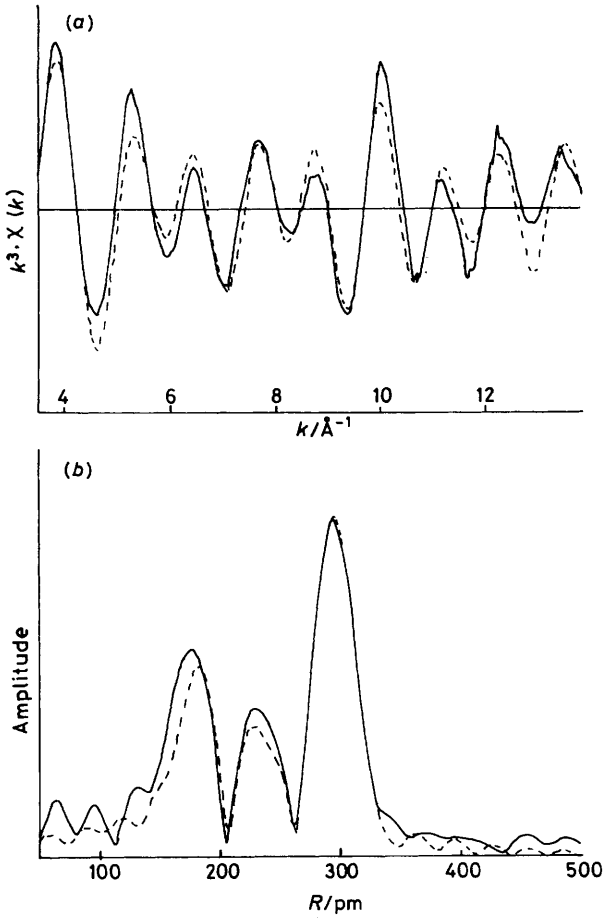

Figure 5. (*a*) k^3-Weighted Ru *K*-edge EXAFS of complex (**1**)–alumina, and (*b*) its Fourier transform. Experimental (——) and calculated (– – –)

Table 1. Ru *K*-edge EXAFS derived distances and Debye–Waller factors for $[Ru_3(CO)_{12}]$ (**2**), (**1**), and (**1**)–alumina: $\alpha = 2\sigma^2$, σ^2 = mean square variation in interatomic distance. *X*-Ray diffraction distances are given in square brackets. Co-ordination numbers were maintained at the crystallographic values for (**2**) and (**3**) [as a model for (**1**)]

	(**2**)	(**1**)	(**1**)–alumina
Ru–C/pm	196 (1) [193][a]	193 (1) [193][b]	190 (1)
α/pm^2	137 (9)	106 (10)	151 (16)
Ru–P/pm		230(1) [229]	229 (1)
α/pm^2		96 (11)	107 (16)
Ru–Ru/pm	284 (1) [287]	283 (1) [285]	275 (1)
α/pm^2	82 (5)	99 (25)	95 (23)
Ru–H–Ru/pm		297 (1) [294]	294 (1)
α/pm^2		87 (11)	106 (15)
Ru···O/pm	296 (1) [299]	296 (1) [306]	290 (1)
α/pm^2	57 (6)	187 (26)	180 (24)
Fit index[c]	1.2	1.4	1.6

[a] Ref. 30. [b] For complex (**3**), ref. 8. [c] Ref. 31.

Table 2. Pentene isomerisation catalysis turnover numbers for (**3**) in solution and (**1**)–alumina at 80 °C for 24 h (e.s.d.s given in parentheses)

Pentene isomer	Conversion	(**3**)	(**1**)–alumina
trans-2-ene	*trans*-1-ene	0.5(1)	0.9(2)
	trans–*cis*	3.3(2)	1.6(2)
cis-2-ene	*cis*–*trans*	9.0(5)	4.5(4)
	cis-1-ene	1.1(1)	0.8(1)
1-ene	1-ene–*trans*	17.0(6)	9.0(3)
	1-ene–*cis*	6.3(5)	4.6(4)

The hydride-bridged ruthenium–ruthenium distance was found to be *ca.* 10 pm longer than the minor non-bridged bond length. Whilst this is near the limit of differentiable distances for the same back-scattering element, the evidence indicates that both distances can be discerned. Although the largest inter-parameter correlation is between *R*(Ru–Ru) and *R*(Ru–H–Ru), at 0.72 it is within the guidelines previously suggested for differentiating subshells.[31] The errors associated with the less populated Ru–Ru shell are larger and this is reflected in the shape of a contour map of the EXAFS fit index for these two most highly correlated parameters [Figure 4(*a*)]. This demonstrates a clear minimum with the larger uncertainty in the minor shell. This split metal shell is a clear indication of the expected isosceles metal triangle expected for this cluster.

The same analytical procedure was adopted for the data obtained on an alumina supported version of (**1**), with the results being presented in Table 1 and Figure 5. The same five-shell model proved the most appropriate; attempts to introduce an oxygen shell to replicate a Ru–O link to the surface were unsuccessful, giving further evidence for the silyl group being the point of attachment to the surface. Most of the shells were refined as having slightly shorter distances for ruthenium in the tethered version of (**1**). Once again there are two metal distances. The separation of 20 pm is greater than in sample (**1**) as can be seen from the more symmetrical form of the fit index contour map [Figure 4(*b*)] indicating less parameter correlation. The environment of an alumina surface clearly affords some contraction of the cluster geometry.

Catalysis by (**3**) *in Solution and on* (**1**)*–Alumina.*—As a test reaction for catalytic activity, the interconversion of the three isomers of n-pentene was investigated using $[Ru_3(\mu\text{-}H)_2(CO)_9(\mu_3\text{-}PPh)]$ (**3**) as the catalyst source. Little activity was observed after 24 h at 50 °C, the cluster being approximately quantitatively recovered. Activity was observed at 110 °C using any of the three isomers as substrate, but only 25% of (**3**) could then be recovered. The best compromise conditions were obtained at 80 °C at which point activity was observed and recovery of the cluster was *ca.* 50%. The activity seems to be linked to the concentration of (**3**), rather than that of one of the decomposition products since the activity is reduced slightly over the first few hours of reaction. This was shown by monitoring the activity for the *cis* to *trans* isomerisation at 100 °C. The mean turnover rate (h^{-1}) was 2.6(3) after 1 h, but reduced monotonically to 1.8(1) after 5 h.

The results of the pentene isomerisation activities are presented in Table 2. These may be compared with the values obtained for a sample of (**1**)–alumina obtained under analogous conditions. The behaviour is approximately parallel, with the activity of the supported cluster being *ca.* 60% that of the dissolved derivative. While the substituents on phosphorus differ between the supported and dissolved species, it seems probable that this reduction may be due to restricted access for the pentene to the cluster when near the oxide surface. There will be little change in the steric effects on changing an alkyl for an

aryl group at phosphorus, with all the other ligands remaining unchanged, and there is only a small difference in the CO stretching frequencies (*ca.* 3—4 cm^{-1}) so the electronic change at ruthenium is probably also small. Reductions in activity on tethering complexes have been noted previously.[5] Following the catalysis, species (**1**) is the only i.r. chromophore in the C–O stretching region. Some decomposition is evident however by the colour change from yellow to beige. Repeating the catalyst cycle for two further runs at 80 °C causes an activity reduction to *ca.* one third of the initial value and a further darkening of the sample. An additional broad i.r. band at 1 970 cm^{-1} is also evident at this stage. Catalysis again seems to follow the concentration of the cluster species.

Conclusions

This work shows that a phosphinidene stabilised cluster with a hydrolysable silyl group can be prepared and tethered to an oxide surface with high specificity. By using a combination of spectroscopic techniques, considerable detail about the structure may be obtained, even when the cluster is bound to an amorphous support. The face-bridging ligand retards, but does not eliminate, cluster breakdown, as evidenced by the higher stability of this material as compared with other triruthenium clusters tethered by terminal or edge bridging ligands.[17,32]

Acknowledgements

We wish to thank the S.E.R.C. for access to the Daresbury Laboratory facilities and for support (to N. B., S. L. C., R. J. P., and D. J. S.). We also thank Shell for a Research Fellowship (to N. J. C.) and other support (to V. D. A.) and Johnson Matthey for the loan of ruthenium salts. We are grateful to Dr. L. M. Moroney for access to her EXAFS background subtraction program.

References

1 S. C. Brown and J. Evans, *J. Chem. Soc., Chem. Commun.*, 1978, 1063.
2 R. Pierantozzi, K. J. McQuade, B. C. Gates, M. Wolf, H. Knözinger, and W. Ruhmann, *J. Am. Chem. Soc.*, 1979, **101**, 5436.
3 J. L. Bilhou, V. Bilhou-Bougnol, W. F. Graydon, J. M. Basset, and A. K. Smith, *J. Mol. Catal.*, 1980, **8**, 411.
4 D. K. Liu and M. S. Wrighton, *J. Am. Chem. Soc.*, 1982, **104**, 898.
5 S. C. Brown and J. Evans, *J. Mol. Catal.*, 1981, **11**, 143.
6 M. B. Freeman, M. A. Patrick, and B. C. Gates, *J. Catal.*, 1982, **73**, 82.
7 R. C. Ryan and C. U. Pittman, *J. Am. Chem. Soc.*, 1977, **99**, 1986.
8 F. Iwasaki, M. J. Mays, P. R. Raithby, P. L. Taylor, and P. J. Wheatley, *J. Organomet. Chem.*, 1981, **213**, 185.
9 S. L. Cook and J. Evans, *J. Chem. Soc., Chem. Commun.*, 1983, 713.
10 D. K. Liu, M. S. Wrighton, D. R. McKay, and G. E. Maciel, *Inorg. Chem.*, 1984, **23**, 212.
11 V. D. Alexiev, N. J. Clayden, S. L. Cook, C. M. Dobson, J. Evans, and D. J. Smith, *J. Chem. Soc., Chem. Commun.*, 1986, 938.
12 S. L. Cook, J. Evans, and G. N. Greaves, *J. Chem. Soc., Chem. Commun.*, 1983, 1287.
13 N. Binsted, S. L. Cook, J. Evans, and G. N. Greaves, *J. Chem. Soc., Chem. Commun.*, 1985, 1103.
14 V. D. Bianco and S. Dorronzo, *Inorg. Synth.*, 1976, **16**, 161.
15 S. L. Cook, J. Evans, L. R. Gray, and M. Webster, *J. Chem. Soc., Dalton Trans.*, 1986, 2149.
16 C. R. Eady, P. F. Jackson, B. F. G. Johnson, J. Lewis, M. C. Malatesta, M. McPartlin, and W. J. H. Nelson, *J. Chem. Soc., Dalton Trans.*, 1980, 383.
17 J. Evans and B. P. Gracey, *J. Chem. Soc., Chem. Commun.*, 1983, 247.
18 S. A. MacLaughlin, A. J. Carty, and N. J. Taylor, *Can. J. Chem.*, 1982, **60**, 87.
19 N. M. Boag, C. E. Kampe, Y. C. Lin, and H. D. Kaesz, *Inorg. Chem.*, 1982, **21**, 1706.
20 M. J. Mays, P. R. Raithby, P. L. Taylor, and K. Henrick, *J. Chem. Soc., Dalton Trans.*, 1984, 959.
21 M. Valle, D. Osella, and G. A. Vaglio, *Inorg. Chim. Acta*, 1976, **20**, 213.
22 S. L. Cook, J. Evans, G. S. McNulty, and G. N. Greaves, *J. Chem. Soc., Dalton Trans.*, 1986, 7.
23 L. M. Moroney, unpublished work.
24 R. J. Price, Ph.D. Thesis, University of Southampton, 1987.
25 S. J. Gurman, N. Binsted, and I. Ross, *J. Phys. C*, 1984, **17**, 143.
26 J. S. Field, R. J. Haines, and D. N. Smit, *J. Organomet. Chem.*, 1982, **224**, C49.
27 M. I. Bruce, D. C. Kehoe, J. G. Matisons, B. K. Nicholson, P. H. Rieger, and M. L. Williams, *J. Chem. Soc., Chem. Commun.*, 1982, 442.
28 S. C. Brown, J. Evans, and L. E. Smart, *J. Chem. Soc., Chem. Commun.*, 1980, 1021.
29 K. Yvon, W. Jeitschko, and E. Parthe, LAZY PULVERIX, University of Geneva, 1977.
30 M. R. Churchill, F. J. Hollander, and J. P. Hutchinson, *Inorg. Chem.*, 1977, **16**, 2655.
31 N. Binsted, S. L. Cook, J. Evans, G. N. Greaves, and R. J. Price, *J. Am. Chem. Soc.*, 1987, **109**, 3669.
32 J. Evans and B. P. Gracey, *J. Chem. Res.*, 1986, (*S*) 42; (*M*) 0601.

Received 30*th December* 1987; *Paper* 7/2272